LIDAR-DERIVED ELEVATION DATA FOR COLUMBIA GLACIER TERMINUS AND ADJACENT SLOPE, SOUTHCENTRAL ALASKA, COLLECTED SEPTEMBER 18, 2022

Katreen M. Wikstrom Jones, Gabriel J. Wolken, and Ronald P. Daanen

Raw Data File 2023-16

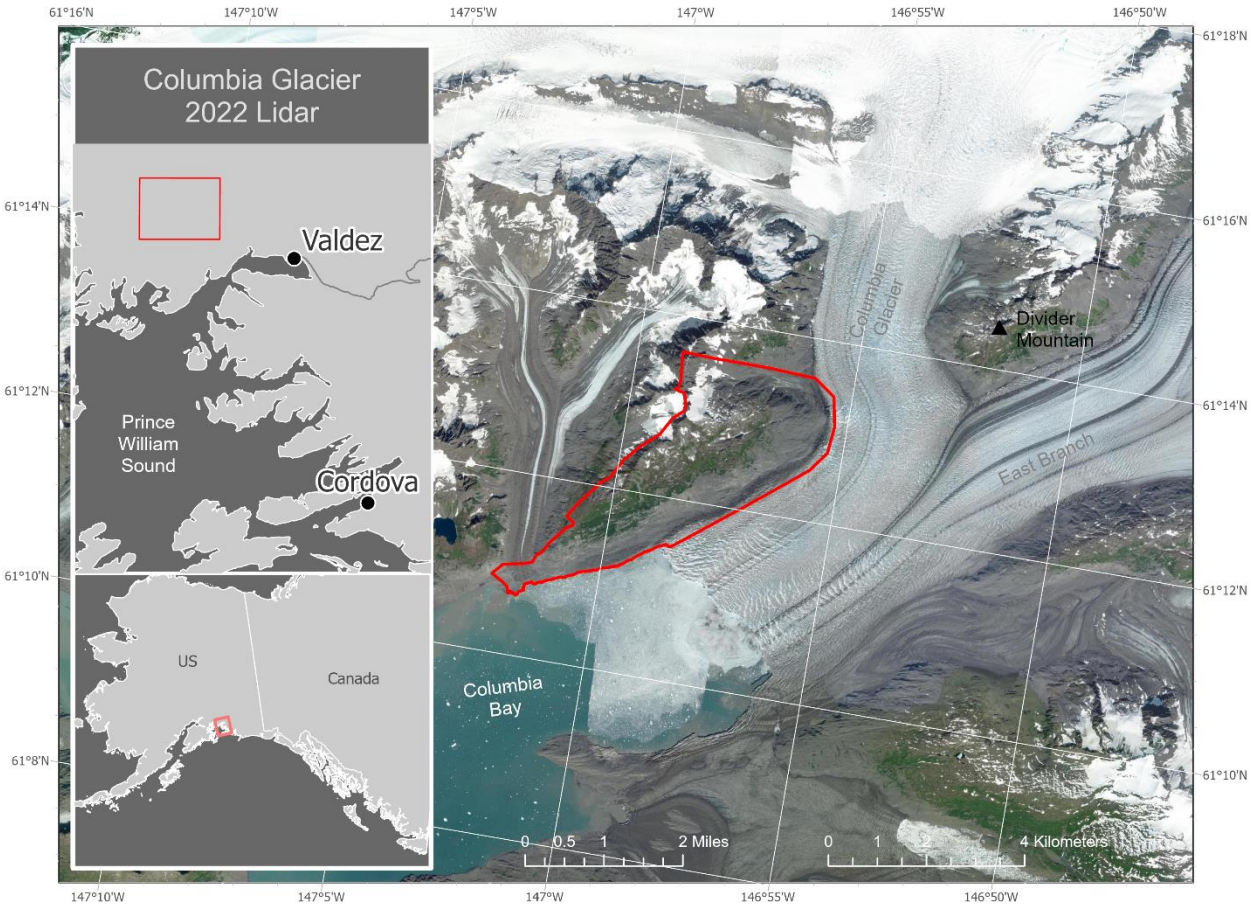

Location map of survey area with orthometric image.

This report has not been reviewed for technical content or
for conformity to the editorial standards of DGGS.

2024
STATE OF ALASKA
DEPARTMENT OF NATURAL RESOURCES
DIVISION OF GEOLOGICAL & GEOPHYSICAL SURVEYS

STATE OF ALASKA
Mike Dunleavy, Governor

DEPARTMENT OF NATURAL RESOURCES
John Boyle, Commissioner

DIVISION OF GEOLOGICAL & GEOPHYSICAL SURVEYS
Melanie Werdon, State Geologist & Director

Publications produced by the Division of Geological & Geophysical Surveys are available to download from the DGGS website (dggs.alaska.gov). Publications on hard-copy or digital media can be examined or purchased in the Fairbanks office:

Alaska Division of Geological & Geophysical Surveys (DGGS)
3354 College Road | Fairbanks, Alaska 99709-3707
Phone: 907.451.5010 | Fax 907.451.5050
dggspubs@alaska.gov | dggs.alaska.gov

DGGS publications are also available at:

Alaska State Library, Historical
Collections & Talking Book Center
395 Whittier Street
Juneau, Alaska 99801

Alaska Resource Library and
Information Services (ARLIS)
3150 C Street, Suite 100
Anchorage, Alaska 99503

Suggested citation:
Wikstrom Jones, K.M., Wolken, G.J., and Daanen, R.P., 2024, Lidar-derived elevation data for Columbia Glacier terminus and adjacent slope, Southcentral Alaska collected September 18, 2022: Alaska Division of Geological & Geophysical Surveys Raw Data File 2023-16. 11 p. https://doi.org/10.14509/31032

In Memorial

Ronnie Daanen, along with colleagues Justin Germann and Tori Moore and pilot Tony Higdon, passed away in July 2023 in a helicopter crash while conducting fieldwork supporting DGGS's mission on the North Slope. This publication is released in their memory.

LIDAR-DERIVED ELEVATION DATA FOR COLUMBIA GLACIER NEAR-TERMINUS UNSTABLE SLOPE, SOUTHCENTRAL ALASKA, COLLECTED SEPTEMBER 18, 2022

Katreen M. Wikstrom Jones[1], Gabriel J. Wolken[1], and Ronald P. Daanen[1]

INTRODUCTION

The Alaska Division of Geological & Geophysical Surveys (DGGS) used aerial lidar to produce a classified point cloud, a digital terrain model (DTM), and an intensity model of the unstable slope at the terminus of Columbia Glacier, located in Prince William Sound in Southcentral Alaska. Aerial and ground control data were collected on September 18, 2022, and subsequently processed in a suite of geospatial processing software. These data support a paraglacial rock slope destabilization study at Columbia Glacier and will be used to assess and characterize an ongoing landslide hazard. This data collection is released as a Raw Data File with an open end-user license. All files are available at https://doi.org/10.14509/31032.

LIST OF DELIVERABLES

Classified Points

DTM

Intensity Image

Metadata

MISSION PLAN

Aerial Lidar Survey Details

DGGS used a Riegl VUX1-LR laser scanner integrated with a global navigation satellite system (GNSS) and Northrop Grumman LN-200C inertial measurement unit (IMU). The lidar integration system was designed by Phoenix LiDAR Systems. The sensor can collect up to 820,000 points per second at a range of up to 150 m. The scanner operated with a pulse repetition rate of 100,000–400,000 pulses per second at a scan rate between 80 and 160 revolutions per second. We used a Cessna 180 fixed-wing platform to survey from an elevation of ~100–500 m above ground level, at a ground speed of ~37 m/s, and with a scan angle set from 80 to 280 degrees. The total survey area covers ~14 km^2 (fig. 1).

Weather Conditions and Flight Times

We flew the aerial survey on September 18, 2022, beginning at 10:21 am and ending at 11:57 am (AKDT). The weather throughout the survey was clear, with still winds.

[1] Alaska Division of Geological & Geophysical Surveys, 3354 College Road, Fairbanks, Alaska 99709

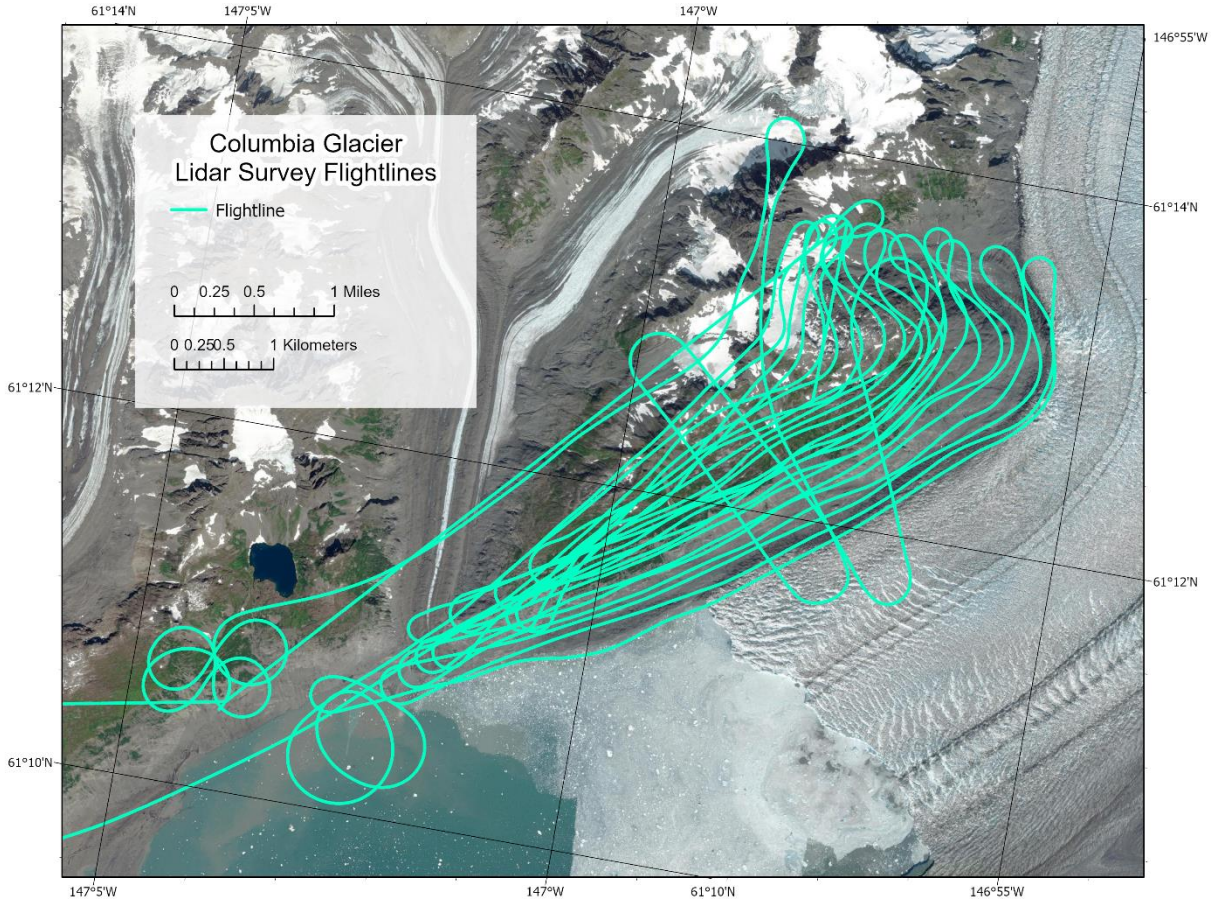

Figure 1. Project flightlines.

PROCESSING REPORT

Lidar Dataset Processing

The point data were processed in SDCimport software for initial filtering and multiple-time-around (MTA) disambiguation. MTA errors, corrected in this process, result from ambiguous interpretations of received pulse time intervals and occur more frequently with higher pulse refresh rates. The IMU and GNSS data were processed in Inertial Explorer, and Spatial Explorer software was used to integrate flightline information with the point cloud. We calibrated the point data at an incrementally precise scale of sensor movement and behavior, incorporating sensor velocity, roll, pitch, and yaw fluctuations throughout the survey. For the lidar data collection, the average nominal pulse density is 31.4 points/m^2 and the average nominal pulse spacing is 17.9 cm.

We created macros in Terrasolid software and classified points in accordance with the American Society for Photogrammetry and Remote Sensing (ASPRS) 2019 guidelines (table 1;

ASPRS 2019). Once classified, we applied a geometric transformation and converted the points from ellipsoidal heights to GEOID12B (Alaska) orthometric heights.

ArcGIS Pro was used to derive raster products from the point cloud. The 0.20-meter DTM was interpolated from all ground class returns using a triangulated-irregular network (TIN) method and minimum values. In ArcGIS Pro, we produced a 0.5-meter intensity image by binning and averaging ground and unclassified points, which include vegetation points.

Classified Point Cloud

Classified point cloud data are provided in compressed LAZ format. This dataset only includes ground points and unclassified points; low- and high-noise points are excluded. Potential vegetation points remain within the unclassified points class. For classified ground points, the average point density is 13.9 points/m^2 (fig. 2).

Table 1. Point cloud class code definitions.

Class Code	Description
1	Unclassified
2	Grounds

Digital Terrain Models

The DTM represents bare earth elevations, excluding vegetation, bridges, buildings, etc. The DTM is a single-band, 32-bit float GeoTIFF file of 0.20-meter resolution. No Data value is set to -3.40282306074e+38.

Lidar Intensity Image

The lidar intensity image describes the relative amplitude of reflected signals contributing to the point cloud. Lidar intensity is largely a function of scanned object reflectance in relation to the signal frequency, is dependent on ambient conditions, and is not necessarily consistent between separate scans. The intensity image is a single-band, 32-bit float GeoTIFF file of 0.5-meter resolution. No Data value is set to -3.40282306074e+38.

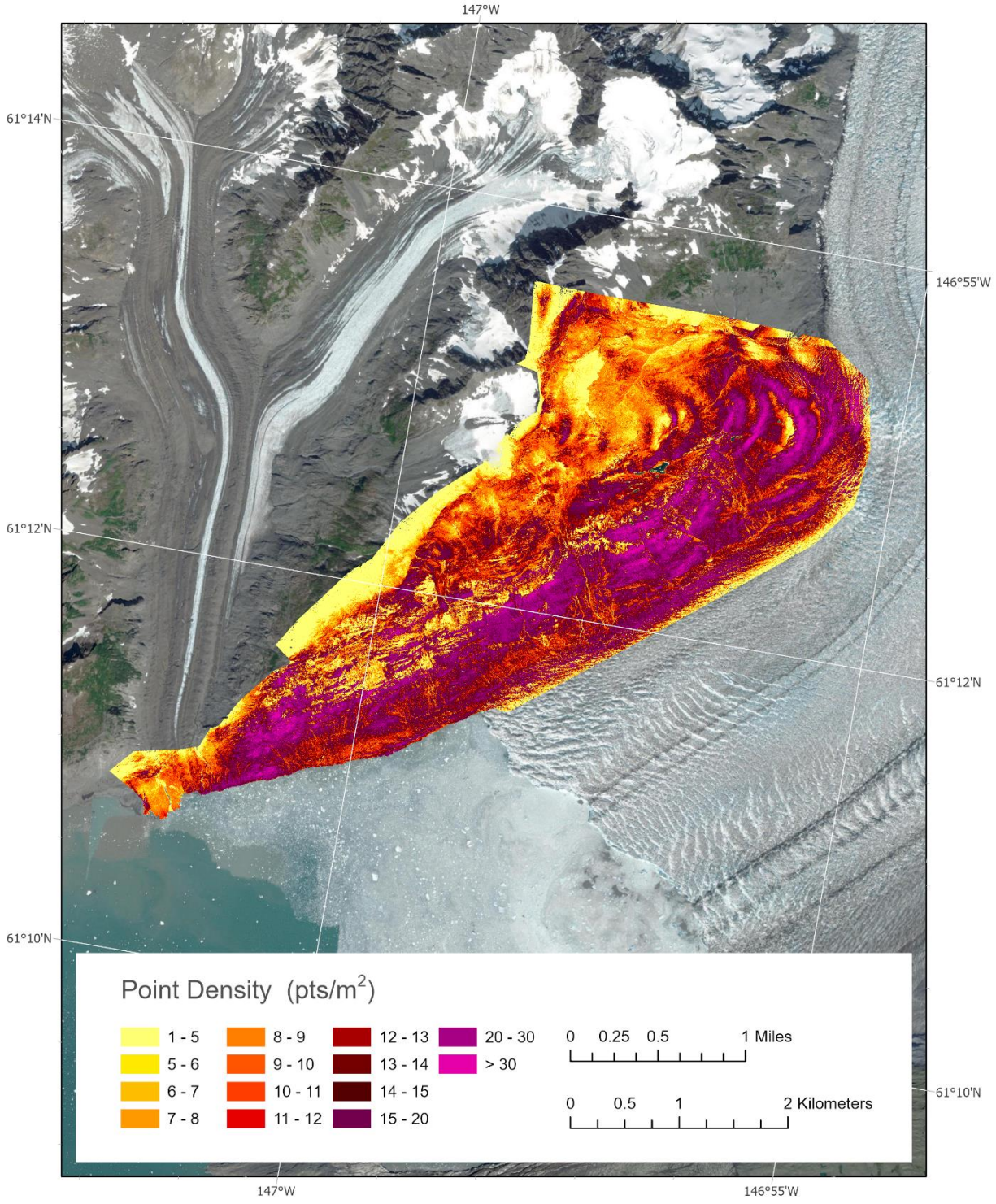

Figure 2. Ground point density for the survey displayed as a 1-meter raster.

SURVEY REPORT

Ground Survey Details

Ground control and check points were collected on September 18, 2022. We deployed a Trimble R10-2 GNSS receiver with an internal antenna at a temporary benchmark at a centralized location within the survey area (61° 12' 37.84428"N; 146° 57' 58.96235"W). It provided a base station occupation and real-time kinematic (RTK) corrections to points we surveyed with a rover Trimble R10-2 GNSS receiver (internal antenna). A total of 82 ground control and check points were collected to use for calibration and to assess the vertical accuracy of the point cloud. All points were collected on bare earth.

Coordinate System and Datum

All data were processed and delivered in NAD83 (2011) UTM6N and vertical datum NAVD88 GEOID12B.

Horizontal Accuracy

Horizontal accuracy was not measured for this collection.

Vertical Accuracy

A mean vertical offset of 19.8 cm was measured between 64 control points and the point cloud (app. 1). A final accuracy of -6.4 cm was achieved by performing a vertical transformation of the lidar point data. Eighteen check points were used to determine the non-vegetated vertical accuracy of the point cloud ground class, using a Triangulated Irregular Network (TIN)-based approach, and a root mean square error (RMSE) of 13.4 cm was achieved (app. 2). We evaluated the relative accuracy for this dataset as the interswath overlap consistency and measured it at 1.9 cm RMSE.

Data Consistency and Completeness

This publication is a complete release dataset. There was no over-collect except for aircraft turns that were eliminated from the dataset. The data quality is consistent throughout the survey.

ACKNOWLEDGMENTS

These data products were funded by a U.S. Geological Survey Cooperative Agreement (Grant Number G21AC10362-00) and the State of Alaska and collected and processed by DGGS. We thank Clearwater Air for their aviation expertise and contribution to these data products. The views and conclusions contained in this document are those of the authors and should not be interpreted as necessarily representing the official policies, either expressed or implied, of the U.S. Government.

REFERENCES

The American Society for Photogrammetry & Remote Sensing (ASPRS), 2019, LAS Specification 1.4 - R15. https://www.asprs.org/wp-content/uploads/2019/07/LAS_1_4_r15.pdf

APPENDIX 1: GROUND CONTROL POINTS

Ground Control Point	Easting (m)	Northing (m)	Known Z (m)	Laser Z (m)	Elevation Difference dZ (Laser Z – Known Z) (m)
1	501793.869	6786212.089	810.224	810.46	0.236
2	501776.001	6786158.791	812.055	812.25	0.195
3	501742.591	6786128.455	807.346	807.61	0.264
4	501775.82	6786124.138	806.78	806.97	0.19
5	501781.754	6786122.794	806.684	806.97	0.286
6	501788.41	6786124.062	807.271	807.48	0.209
7	501813.353	6786119.378	809.551	809.76	0.209
8	501847.737	6786142.527	804.517	804.62	0.103
9	501865.317	6786154.74	804.029	804.29	0.261
10	501897.589	6786156.904	802.627	802.84	0.213
11	501902.978	6786148.2	801.015	801.23	0.215
12	501916.463	6786146.926	799.758	800	0.242
13	501918.282	6786159.518	799.921	800.02	0.099
14	501920.153	6786170.865	799.694	799.88	0.186
15	501916.126	6786193.124	802.37	802.46	0.09
16	501958.032	6786229.679	803.484	803.73	0.246
17	501970.386	6786234.556	805.423	805.67	0.247
18	502018.989	6786190.071	822.582	822.83	0.248
19	502091.496	6786258.836	817.681	817.6	-0.081
20	502122.757	6786290.001	806.282	806.35	0.068
21	502155.899	6786302.986	808.673	808.98	0.307
22	502185.219	6786305.919	812.395	812.54	0.145
23	502204.192	6786311.696	808.55	808.67	0.12
24	502235.09	6786348.614	806.939	807.2	0.261
25	502260.265	6786347.582	802.954	803.2	0.246
26	502272.128	6786356.813	804.301	804.6	0.299
27	502291.346	6786372.518	802.619	802.88	0.261
28	502296.611	6786364.845	800.638	800.86	0.222
29	502320.752	6786367.437	798.227	798.31	0.083
30	502351.85	6786372.196	795.028	795.03	0.002
31	502382.055	6786386.203	784.785	785.06	0.275
32	502452.143	6786434.668	764.845	765.02	0.175
33	502459.777	6786440.654	764.668	764.78	0.112
34	502431.072	6786490.836	783.649	783.79	0.141
35	502425.686	6786492.47	784.694	784.83	0.136
36	502418.899	6786515.074	790.121	790.27	0.149
37	502417.635	6786534.143	789.849	790.12	0.271
38	502430.942	6786569.079	797.959	798.09	0.131

Ground Control Point	Easting (m)	Northing (m)	Known Z (m)	Laser Z (m)	Elevation Difference dZ (Laser Z – Known Z) (m)
39	502438.964	6786605.198	802.463	802.5	0.037
40	502445.027	6786602.101	802.667	802.78	0.113
41	502464.676	6786582.271	801.52	801.83	0.31
42	502456.857	6786578.433	802.426	802.35	-0.076
43	502399.023	6786525.289	789.815	790.13	0.315
44	502370.922	6786496.656	796.02	796.24	0.22
45	502229.655	6786419.135	818.672	818.68	0.008
46	502221.007	6786425.551	819.616	819.88	0.264
47	502165.291	6786417.56	816.463	816.92	0.457
48	502151.515	6786407.598	818.812	819.14	0.328
49	502094.523	6786407.128	818.829	818.95	0.121
50	502027.245	6786403.125	819.526	819.71	0.184
51	502033.914	6786403.114	818.834	819.12	0.286
52	501986.918	6786388.083	825.676	825.85	0.174
53	501932.589	6786347.528	826.53	826.73	0.2
54	501899.698	6786331.179	824.109	824.5	0.391
55	501856.202	6786308.637	817.71	817.94	0.23
56	501826.457	6786277.735	813.153	813.47	0.317
57	501774.604	6786226.474	813.241	813.48	0.239
58	501767.656	6786227.69	813.778	813.92	0.142
59	501799.16	6786228.804	814.27	814.48	0.21
60	501695.345	6786249.045	826.476	826.7	0.224
61	501618.293	6786329.493	880.815	880.77	-0.045
62	501656.157	6786350.093	878.169	878.58	0.411
63	501745.33	6786381.006	887.15	887.38	0.23
64	501744.109	6786384.689	887.249	887.54	0.291
Average Elevation Difference (dZ) (m)	0.198				
Minimum dZ (m)	-0.081				
Maximum dZ (m)	0.457				
Average magnitude error (m)	0.204				
Root mean square error (m)	0.224				
Standard deviation (m)	0.107				

APPENDIX 2: CHECK POINTS

Check Point	Easting (m)	Northing (m)	Known Z (m)	Laser Z (m)	Elevation Difference dZ (Laser Z – Known Z) (m)
1	501799.131	6786228.814	814.275	814.26	-0.015
2	501768.891	6786124.289	806.903	806.99	0.087
3	501826.305	6786128.599	810.253	810.02	-0.233
4	501911.986	6786146.133	799.557	799.6	0.043
5	501947.221	6786235.375	802.52	802.58	0.06
6	502096.651	6786268.572	812.343	812.21	-0.133
7	502218.096	6786315.179	805.04	805.06	0.02
8	502290.609	6786367.555	802.033	801.93	-0.103
9	502363.095	6786384.948	789.375	789.15	-0.225
10	502464.157	6786442.729	764.079	763.9	-0.179
11	502439.15	6786560.702	797.972	797.95	-0.022
12	502462.635	6786596.191	802.687	802.69	0.003
13	502296.681	6786446.48	805.842	805.87	0.028
14	502097.237	6786407.211	818.594	818.51	-0.084
15	501968.052	6786368.685	828.341	828.43	0.089
16	501809.492	6786263.158	812.444	812.45	0.006
17	501619.534	6786330.801	880.924	880.68	-0.244
18	501757.01	6786381.725	885.498	885.24	-0.258
Average Elevation Difference dZ (m)	-0.064				
Minimum dZ (m)	-0.258				
Maximum dZ (m)	0.089				
Average magnitude error (m)	0.102				
Root mean square error (m)	0.134				
Standard deviation (m)	0.12				